Ionics (2011) 17:399–405
DOI 10.1007/s11581-011-0524-8

ORIGINAL PAPER

Effects of various $LiPF_6$ salt concentrations on PEO-based solid polymer electrolytes

**Suriani Ibrahim · Mariah Mohd Yassin ·
Roslina Ahmad · Mohd Rafie Johan**

Received: 8 November 2010 / Accepted: 16 January 2011 / Published online: 8 February 2011

Abstract In this research, various weight percents of $LiPF_6$ are incorporated into PEO-based polymer electrolyte system. Thin film electrolytes are prepared via solution casting technique and characterized by FTIR, XRD and DSC analyses in order to study their complex behaviour. The amorphicity of the electrolytes are measured by DC impedance. The results reveal that the conductivity increases with increasing temperature when the salt concentration increases to 20 wt.%. The conductivity for 20 wt.% of salt remains similar to the conductivity of 15 wt.% of salt at 318 K. Impedance studies show that the conductivity increases with increasing $LiPF_6$ concentration, whereas XRD studies reveal that the phase changes from crystalline to amorphous when $LiPF_6$ concentration increases. DSC studies indicate a decrease in T_m with increasing $LiPF_6$ concentration. Finally, the complexation process is examined using FTIR.

Keywords Polyethylene oxide (PEO) · Lithium hexafluorophosphate ($LiPF_6$) · Solid polymer electrolyte · Ionic conductivity

Introduction

Solid polymer electrolytes (SPE) currently receive a great deal of attention because of their proposed large-scale use in secondary lithium ion batteries [1]. The development of SPE has drawn much interest among researchers [2–4]. The high molecular weight polyethylene oxide (PEO)-based composite polymer electrolytes are gaining popularity as the best candidates for polymer matrix due to their salvation power, complexation ability and ion transport mechanism directly connected to the alkaline cell [5]. The desirable characteristics of SPE are: good compatibility with lithium metal, no leakage, low self-discharge in batteries, elastic relaxation under stress, ease in processing and continuous production [6, 7]. However, the low ionic conductivity of SPE limits their applications. It is known that the ionic transport of SPE occurs only in the amorphous polymer regions and is often governed by the segmental motion of polymer chain [8, 9]. It is clear that the presence of a flexible, amorphous phase in SPE is essential for higher ionic conductivity. Although many kinds of polymeric electrolytes such as poly(acrylonitrile) [10], poly(propylene oxide) [11], poly(methyl methacrylate) [12] and poly (maleic anhydridestyrene) [11] have been studied, high molecular weight PEO-based SPE is actively researched for technological applications and fundamental studies [6, 13].

The high ionic conductivities observed in polymer/alkali metal salt complexes, particularly those involving PEO and lithium salts, have stimulated great interest for all solid-state, high-energy-density batteries [14, 15]. PEO, the most extensively studied polymer, can form complexes with a wide range of metal salts including alkali, alkaline earth and transition metal salts. PEO/salt electrolytes suffer one major drawback, whereby PEO is semi-crystalline at ambient temperature. Much effort has been devoted to solid polymer electrolytes in order to understand the mechanisms and governing structure of polymer electrolytes and their ability to solvate ions and yield high ionic conductivity. Several salts have been used to increase the conductivity of polymer electrolytes such as $Mg(NO_3)_2$ [16], $LiCF_3SO_3$ [17], KI [18], $NaClO_3$ [19] and $LiPF_6$ [20]. From the

S. Ibrahim (✉) · M. M. Yassin · R. Ahmad · M. R. Johan
Advanced Materials Research Laboratory, Department of Mechanical Engineering, Faculty of Engineering,
University of Malaya,
50603 Kuala Lumpur, Malaysia
e-mail: sue_83@um.edu.my

various salts mentioned, lithium hexafluorophosphate ($LiPF_6$) remains the only salt used in practical lithium ion batteries [21]. The conductivity increases with increasing concentrations of $LiPF_6$, up to 15 wt.% concentration. The conductivity for 20 wt.% $LiPF_6$ at room temperature is about 4.10×10^{-5} S cm^{-1}, which is the highest conductivity value reported in the literature [16–20]. In addition, $LiPF_6$ is the most stable salt at room temperature, provided that the amount of H_2O is very low (less than 1 mg L^{-1}) [20]. Owing to the benefits of $LiPF_6$, this paper is focused on the effects of various $LiPF_6$ salt concentrations on the properties of solid polymer electrolytes.

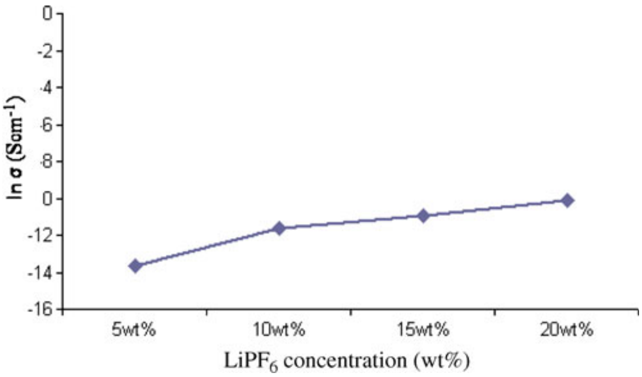

Fig. 1 Variation of conductivity as a function of $LiPF_6$ content at room temperature

Experimental

The electrolytes were prepared using PEO (Aldrich, with an average molecular weight of 6×10^6) which was dried at 50 °C under vacuum for 48 h, and $LiPF_6$ was used without further purification. PEO and various ratios of $LiPF_6$ were composed and dissolved, in sequence, with acetonnitrile and are listed in Table 1. The mixture was stirred for 24 h, and the resulting solution was poured into a petri dish. The solvent was left to evaporate at room temperature. The prepared electrolytes were subjected to several characterization studies. Conductivity studies were carried out using HIOKI 3532–50 LCR HiTESTER, and differential scanning calorimetry (DSC) thermographs were obtained using DSC 820 fitted with 56 thermocouples. Fourier transform infrared spectroscopy (FTIR) spectra were obtained using Perkin Elmer Spectrum 400, and X-ray diffraction (XRD) analysis was conducted using Bruker model D8 Advance.

Results and discussion

Conductivity studies

Figure 1 shows the variation of room temperature conductivity as a function of salt concentration. The dependence of conductivity on salt concentration provides information on the specific interaction between salt and the polymer matrix. It is observed that the conductivity increases upon the addition of salt. The highest conductivity is obtained at 4.1×10^{-5} S cm^{-1} for 20 wt.% of $LiPF_6$. The conductivity is expected to decrease beyond 20 wt.% of $LiPF_6$ due to a decrease in the number of charge carriers which lower the segmental motion of the polymer chain [18].

Table 1 Thermal properties of salted polymer electrolyte

Sample	T_m (°C)	ΔH_m (Wg^{-1})	X_c (%)
PEO	69	9.00	100
PEO–5 wt.% $LiPF_6$	72	20.1	183
PEO–10 wt.% $LiPF_6$	66	7.20	179
PEO–15 wt.% $LiPF_6$	66	15.3	139
PEO–20 wt.% $LiPF_6$	59	10.9	106

As the salt content increases, the conductivity increases because the number density of mobile ions increases. Therefore, the polymer segment's motion is promoted [22]. The results agree well with the Rice and Roth model [17, 23]:

$$\sigma = \frac{2}{3}\left[\frac{(Ze)^2}{k_B Tm}\right]\eta E_A \tau \exp\left(-\frac{E_A}{k_B T}\right) \qquad (1)$$

where σ, η, Z, e, E_A and m represent the conductivity, density, charge carrier, elementary charge, activation energy and mass of the conducting ions, respectively. Furthermore, the parameters T, k_B, e and τ represent the absolute temperature, Boltzman constant, electronic charge and time travel of ions between sites, respectively. From Eq. 1, it can be seen that the conductivity increases when the density of mobile ions increases.

Figure 2 shows the complex impedance plot for the PEO–$LiPF_6$ complex at room temperature. The absence of a high-frequency, semi-circular region at a higher salt content verifies that the current carriers are ions. Therefore, the total conductivity of the complexes is mainly due to the ion conduction.

Figure 2a–d shows the complex impedance plots for samples with 0, 5, 10, 15, 20 wt.% $LiPF_6$ at room temperature, respectively. A part of a depressed semicircle can be observed for the sample with 0 wt.% $LiPF_6$. The semicircle can be represented by a parallel combination of a capacitor, which is due to the immobile polymer chain [24]. As the salt concentration begins to increase, the semicircle in the plots is observed to lessen and finally results in a low-frequency spike. This observation suggests that only the resistive component of the polymer electrolytes exists

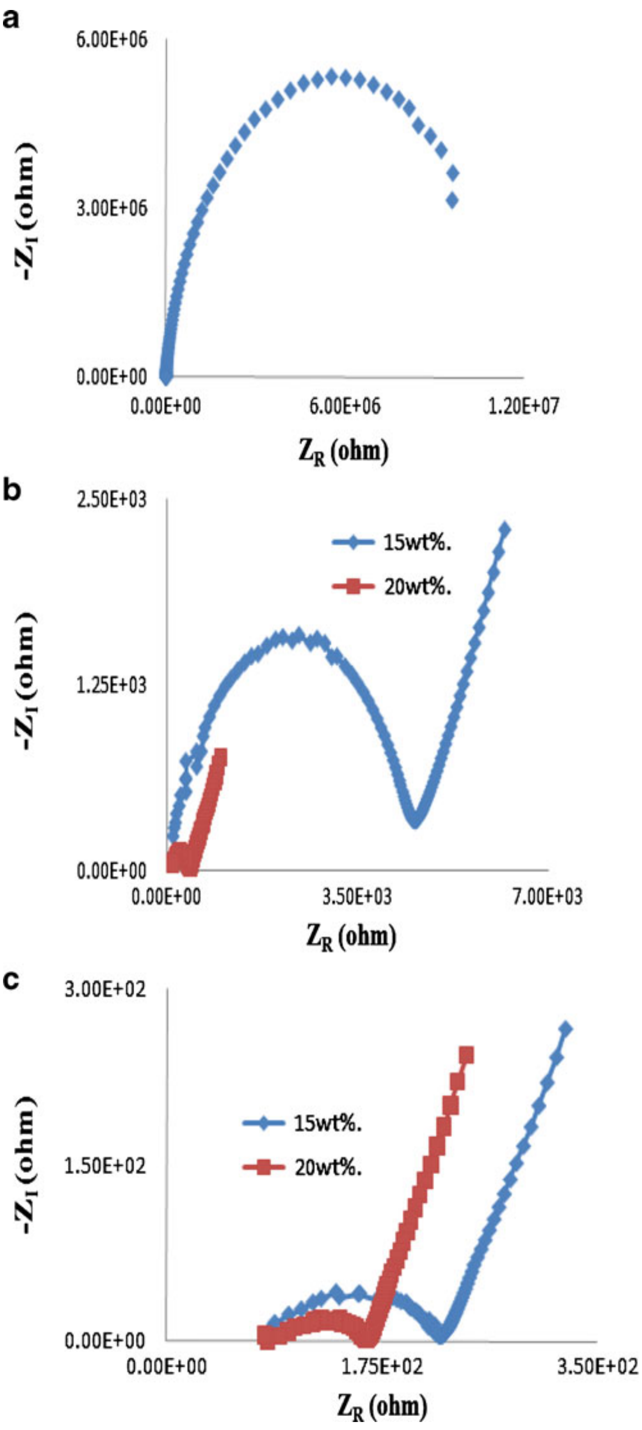

Fig. 2 Impedance plots of samples containing **a** 0 wt.%, **b** 5 wt.%, 10 wt.%, **c** 15 wt.%, 20 wt.%

[24, 25], which is due to the mobile ions inside the polymer matrix.

The R_b for all samples was calculated from the low-frequency intercept of the semicircle or high-frequency intercept of the spike on the real axis. It is found that the R_b decreases with an increase in salt concentration. This may be due to an increase in mobile charge carriers upon the addition of $LiPF_6$. The R_b is obtained to be 5.36×10^6 S cm^{-1}, 4.64×10^3 S cm^{-1}, 5.19×10^2 S cm^{-1}, 2.52×10^2 S cm^{-1} and 1.61×10^2 S cm^{-1} for 0, 5, 10, 15 and 20 wt.% concentration of $LiPF_6$, respectively.

The conductivities of PEO complex films are found to increase with temperature from 303 K to 373 K, and the films are found to be mechanically stable [26]. At higher temperatures, the thermal movement of polymer chain segments and the dissociation of salts improve, which increase conductivity. In the complex impedance plots shown in Fig. 3, the disappearance of a depressed semicircle at high frequencies reveals the absence of capacitive nature, and therefore, only diffusion processes take place [27]. The intercept at the real axis gives the electrolytes' resistance, and the values decrease with increasing sample temperature and ionic mobility. However, the charge concentrations do not necessarily increase with temperature for polymeric electrolytes [23].

Figure 4 shows the Arrhenius plot of ionic conductivity at various weight percents of $LiPF_6$. The temperature dependence of the ionic conductivity is not linear and obeys the Vogel–Tamman–Fulcher (VTF) relationship.

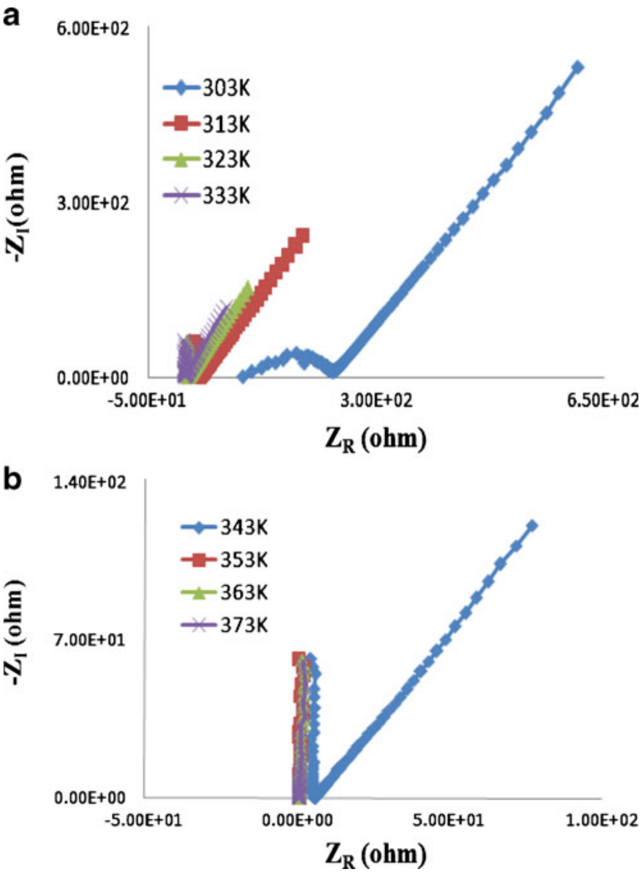

Fig. 3 Impedance plot of samples at temperatures of **a** 303–313 K and **b** 343–373 K

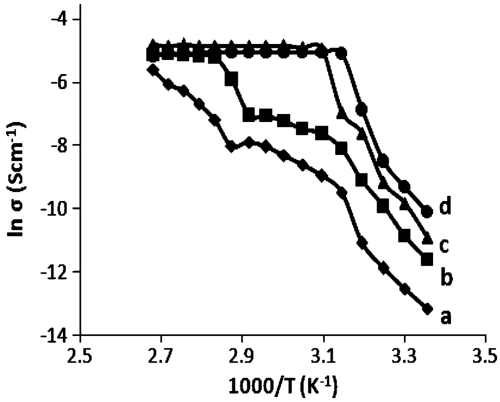

Fig. 4 Conductivity dependence temperature of complexes at various weight percents of $LiPF_6$. **a** 5, **b** 10, **c** 15, **d** 20

In PEO–$LiPF_6$ films, 20 wt.% $LiPF_6$ with PEO is the highest composition of solid films achievable. At higher compositions of $LiPF_6$, films fail to form and remain in a gel-like state. This may be caused by the presence of water molecules. It is known that the $LiPF_6$ salt possesses a high capability to absorb water molecules at high temperatures of approximately 40 °C [20]. Thus, at higher compositions of $LiPF_6$ salt, more moisture is absorbed, which increases the mobility of the PEO–$LiPF_6$ system. Consequently, water molecules form hydrogen bonds with PEO and disrupt the linkage between PEO–$LiPF_6$ systems [17]. To analyse the mechanisms of ionic conduction, PEO–$LiPF_6$ systems were investigated at a temperature range of 298 to 373 K, as shown in Fig. 4.

The initial increase in conductivity is presumably due to an increase in the number of charge carriers in the matrix. For higher concentrations of $LiPF_6$, the charge build-up is offset by the retarding effect of ion aggregates such as ion pairs and ion triplet formation, which causes constraints in ionic and polymer segmental mobility [1]. Hence, the conductivity reaches the maximum value at 20 wt.% $LiPF_6$ complex. This shows a balance between the two opposing forces, which is an increase in the number of charge-carrier ions and a decrease in ionic mobility [1].

Even though pure PEO is an insulator, pure PEO shows a conductivity of 10^{-10} at room temperature. It may be noted that the small value of conductivity in pure polymers is commonly due to the presence of impurities trapped during the preparation of the complex. The polar and flexible PEO main chain dissociates $LiPF_6$ to generate carrier ions, and the migration of these ions through interchain and intrachain polymer segments in the amorphous region of the complex [28] is responsible for the increase in conductivity. The increase of salt concentration above 20 wt.% leads to a decrease in conductivity, which may be due to ion association in the polymer complexes by reducing the availability of vacant coordinating sites [28].

A number of studies have been conducted to investigate PEO used in polymer electrolytes. Ramesh et al. [17] proved that in a PEO–$LiCF_3SO_3$ system, a PEO having 12 wt.% $LiCF_3SO_3$ exhibits the highest conductivity with a value of 1.10×10^{-6} S cm^{-1}, whereas a PEO with 5 wt.% Li_2SO_4 possesses the lowest conductivity with a value of 7.27×10^{-10} S cm^{-1}. Paruthimal et al. [18] investigated PEO complexed with KI salt and obtained a conductivity of about 6.23×10^{-5} S cm^{-1} at 303 K for a molar ratio of 12:1 (PEO/KI) [18]. Siva Kumar et al. [19] studied PEO complexed with $NaClO_3$ and obtained a conductivity value of 3.36×10^{-7} S cm^{-1} at 303 K. In this research, the conductivity for pure PEO is found to be 5.28×10^{-10} S cm^{-1} at 303 K, and the value increases gradually to 6.76×10^{-5} S cm^{-1} when 20% $LiPF_6$ was added into the PEO.

DSC studies

Figure 5 shows the DSC curves of complexes at various weight percents of $LiPF_6$. A sharp endothermic peak was observed at a temperature near 65 °C for pure PEO during

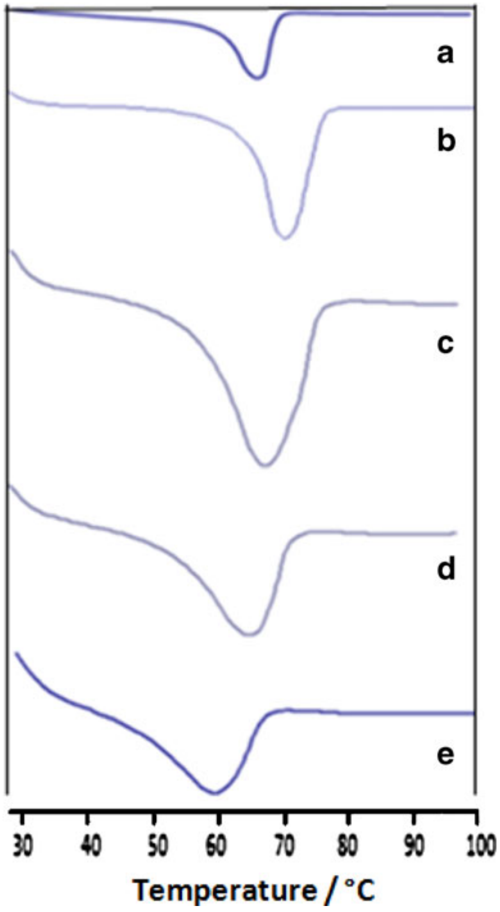

Fig. 5 DSC curves of salted polymer electrolyte at various weight percents of $LiPF_6$. **a** 0, **b** 5, **c** 10, **d** 15, **e** 20

the heating process, as shown in Fig. 5a. The addition of salt causes peak broadening as well as movement of its position to lower temperatures. Table 1 summarizes the DSC results. It shows that the melting temperature of PEO complexes with $LiPF_6$ decreases with increasing $LiPF_6$ concentration. The decrease in PEO melting temperature by $LiPF_6$ addition also indicates the complexation of $LiPF_6$ and PEO. The destruction of PEO crystallinity is clearly observed. This result is also confirmed by the XRD analysis, as shown in Fig. 6.

XRD studies

The X-ray diffractograms for various concentrations of PEO-$LiPF_6$ complexes are shown in Fig. 6. The crystalline nature for each sample is compared with that of pure PEO. Sharp and intense diffraction lines occur at $2u$-20° and 24°, indicating the crystalline nature of pure PEO [23]. The intensities of PEO peaks at $2u$-20° and 24° are observed to decrease upon the addition of salt. However, it can be seen that the diffraction pattern resembles that of pure PEO. The sharpness of the diffraction lines remains unchanged, suggesting that a portion of the PEO remains salt-free, and the other portion of PEO containing salt transforms to an amorphous phase. This indicates that the crystalline

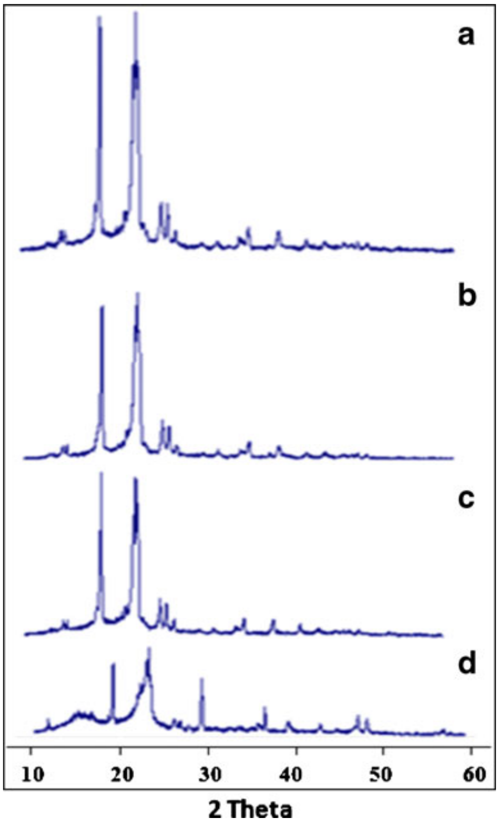

Fig. 6 XRD pattern of salted polymer electrolyte at various weight percents of $LiPF_6$. **a** 5, **b** 10, **c** 15, **d** 20

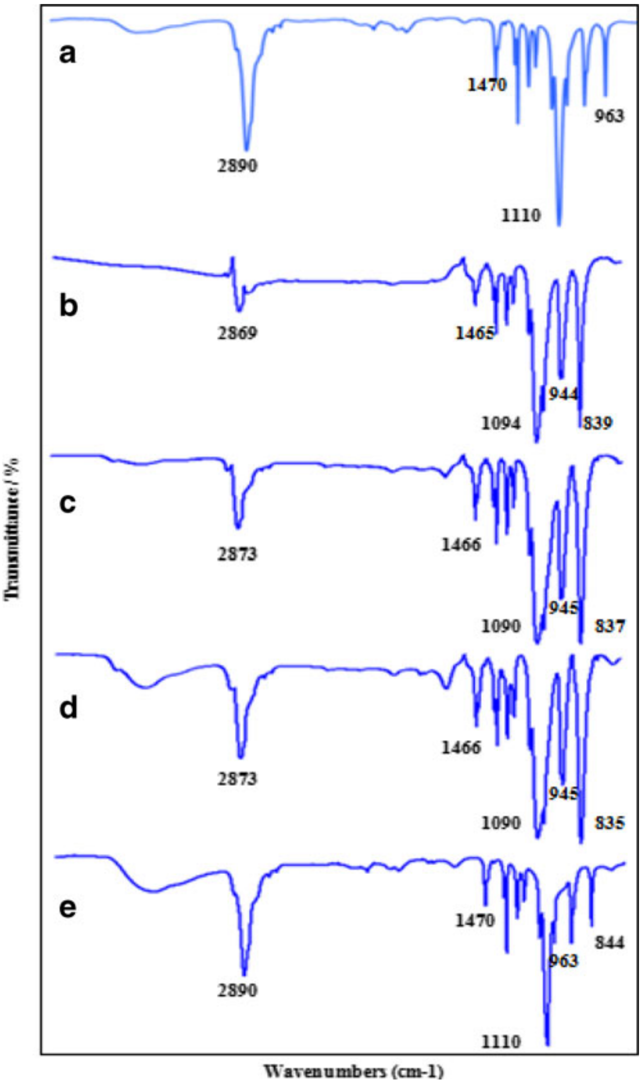

Fig. 7 FTIR spectra of pure PEO and various weight percents of $LiPF_6$ in complexes **a** 0, **b** 5, **c** 10, **d** 15, **e** 20

Table 2 FTIR transmittance bands' positions and their assignments

Material	Vibrational frequency (cm^{-1})	Band assignment
PEO	842,963	CH_2 twisting nagging [30]
	1,100	Anti-symmetric bridge C–O–C stretching [30]
	1,241; 1,280	Asymmetric CH_2 twisting [30]
	1,455	Asymmetric CH_2 [30]
	2,800–1,211	Symmetric C–H stretching [30]
	2,700–2,800	Asymmetric C–H stretching [30]
$LiPF_6$	651	v(PF_6–) [31]
	837	v(PF_6–) [31]
	1,164	v(PF_5) [31]

phase of uncomplexed PEO exists in the solid electrolyte films. As the salt concentration increases, it can be observed that there are changes in $2u$ from $2u$-24° to $2u$-23.3° and $2u$-20° to $2u$-19.2°. In this salt concentration regime, it can be noticed that the intensities of the diffraction peaks at $2u$-23.3° and $2u$-19.2° decrease slightly. Therefore, the angles $2u$-23.3° and $2u$-19.2° appear to be the preferred crystallographic direction, whereby an interaction of PEO and salt takes place. The variation in intensity of the diffraction peaks at different doping salt concentrations from 5 to 20 wt.% of $LiPF_6$ indicates the increase in the number of preferred oriental ions for each concentration, which leads to an increase in electrical conductivity in the salt concentration regime. New peaks at $2u$-29.4° begin to appear in the diffractogram for films with 20 wt.% of $LiPF_6$, showing the formation of a new crystalline phase. The new peaks suggest the formation of crystalline PEO–$LiPF_6$ complexes.

FTIR studies

Figure 7 depicts the IR transmittance spectra of the samples recorded at room temperature in the region of 4,000–500 cm^{-1}. FTIR transmittance bands' positions and assignments of the individual materials are listed in Table 2. It is observed that peaks occur between 4,000–3,100 cm^{-1}, corresponding to the OH group. The peaks broaden with an increase in $LiPF_6$ salt concentration. This is due to the decomposition of $LiPF_6$ to solid LiF and gases of OPF_3 and HF, which is represented by the following equation [29]:

$$LiPF_6 + H_2O \rightarrow LiF(s) + OPF_3(g) + HF(g) \qquad (2)$$

As $LiPF_6$ salt concentration increases, the intensity of symmetric stretching vibration band of pure PEO increases and shifts to 2,869 cm^{-1} (Fig. 6a), 2,873 cm^{-1} (Fig. 6b–c) and 2,890 cm^{-1} (Fig. 6d). This is due to the additional amount of Li^+ in the complexes. The anti-symmetric stretching vibration band at 1,100 cm^{-1} of pure PEO is shifted to 1,094 cm^{-1} (Fig. 6a), 1,090 cm^{-1} (Fig. 6b–c) and 1,110 cm^{-1} (Fig. 6d) as $LiPF_6$ concentration increases. The peaks broaden with the exception of 20 wt.% of $LiPF_6$. This may be due to the ion aggregates such as ion pairs and ion triplet formation, which cause constraints to ions and polymer segmental mobility. This explains the nature of conductivity result for 20 wt.% of $LiPF_6$ shown in Fig. 3. A similar reaction occurs to the twisting vibration bands at 842 and 963 cm^{-1} for pure PEO. When the weight percent of $LiPF_6$ is increased, the peaks are shifted to 839 and 944 cm^{-1} (Fig. 6a), 945 and 837 cm^{-1} (Fig. 6b), 945 and 835 cm^{-1} (Fig. 6c) and 963 and 844 cm^{-1} (Fig. 6d). The peaks' intensities are increased with the exception of 20 wt.% of $LiPF_6$.

Conclusions

PEO-based polymer electrolyte systems with various weight percents of $LiPF_6$ have been synthesized using solution casting technique. The system with 20 wt.% $LiPF_6$ exhibits a maximum conductivity of 10^{-5} S cm^{-1} at room temperature. The temperature dependence of ionic conductivity of the electrolytes obeys the VTF relationship. At the molecular level, FTIR studies provide strong evidence that there is a specific interaction between PEO and $LiPF_6$. The change in peak intensity, shape and position confirms the complexation process of PEO–$LiPF_6$ systems. The DSC curves indicate that the addition of various weight percents of $LiPF_6$ on polymer electrolytes decreases the melting transition temperature (T_m) and degree of crystallinity of the system.

Acknowledgements This work was financially supported by the PPP fund (PS083/2009B) provided by University of Malaya and Science fund (Grant no. 13-02-03-3068) provided by the Ministry of Science, Technology and Environment (MOSTE), Malaysia. We warmly acknowledge Mr. Ismail, Mr. Yap, Mr. Din and Ms. Lina from the Department of Physics, University of Malaya for their assistance during FTIR testing and Mr. Zailan, Mr. Riduan and Dr. Hafiz for their assistance during XRD testing at University Kebangsaan Malaysia. The authors specially thank Ms. Nadia for her constructive comments on the manuscript.

References

1. Rajendran S, Sivakumar P, Shanker Babu R (2007) J Power Sources 164:815–821
2. Teeters D, Robert GN, Brian DT (1996) Solid State Ionics 85:239
3. Sukeshini AM, Kulkarni AR, Sharma A (1998) Solid State Ionics 179:113–115
4. Pitawala HMJC, Dissanayake MAKL, Seneviratne VA (2007) Solid State Ionics 178:885
5. Johan MR, Leo BF (2010) Ionics 16:335–338
6. Lightfoot P, Metha MA, Bruce PG (1993) Science 262:883
7. Xu W, Deng ZH, Zhang XZ, Wan GX (1998) J Solid State Electrochem 2:257
8. Wieczorek W, Raducha D, Zalewska A, Stevens JR (1998) J Phys Chem B 102:8725
9. Chu PP, Jen HP, Lo FR, Lang CL (1999) Macromolecules 32:4738
10. Choe HS, Carroll BG, Pasquariello DM, Abraham KM (1997) Chem Mater 9:369
11. Vachon C, Labreche C, Valle A, Besner S, Dumont M, Prud'homme J (1995) Macromolecules 28:5585
12. Rhoo HJ, Kim HT, Park JK, Hwang TS (1997) Electrochim Acta 42:1571
13. Lee HS, Yang XQ, MacBreen J, Xu ZS, Skotheim TA, Okamoto Y (1994) J Electrochem Soc 141:886
14. Fenton DE, Parker JM, Wright PV (1973) Polymer 14:589
15. Armand MB, Chabagno JM, Duclot M (1979) In: Vashista P, Mundy JN, Shenoy GK (eds) Fast ion transport in solids. North-Holland, Amsterdam, p 131
16. Ramalingaiah S, Srinivas Reddy D, Jaipal Reddy M, Laxminarsaiah E, Subba Rao UV (1996) Mater Lett 29:285–289

17. Ramesh S, Fung Yuen T, Jun Shen C (2008) Spectrochim Acta A 69:670–675
18. Paruthimal KG, Kang M-S, Kang YS (2006) Solid State Ionics 177:1091–1097
19. Siva Kumar J, Subrahmanyam AR, Jaipal Reddy M, Subba Rao UV (2006) Mater Lett 60:3346–3349
20. Teng X-G, Li F-Q, Ma P-H, Ren Q-D, Li S-Y (2005) Thermonhim Acta 436:30–34
21. Cowie JMG (1987) In: MacCallum JR, Vincent CA (eds) Polymer electrolytes reviews. Vol. 1. Applied science. Elsevier, London
22. Rajendran S, Shanker Babu R, Sivakumar P (2007) J Power Sources 170:460–464
23. Ahmad Khiar AS, Arof AK (2010) Ionics 16:123–129
24. Ramesh S, Arof AK (2001) Mater Sci Eng B 85:11–15
25. Baskaran R, Selvasekarapandian S, Kuwata N, Kawamura J, Hattori T (2004) Mater Chem Phys 98:55–61
26. Jaipal Reddy M, Peter Chu P (2002) Electrochim Acta 47:1189–1196
27. Ratner MA, Nitzan A (1989) Faraday Discuss Chem Soc 88:19–42
28. Druger SD, Ratner MA, Nitzan A (1983) Solid State Ionics 9/10:1115
29. Anantha PS, Hariharan K (2005) Solid State Ionics 176:155–162
30. Osman Z, Arof AK (2003) Electrochimica Acta 48:993–999
31. Stygar J, Zukowska G, Wieczorek W (2005) Solid State Ionics 174:2645–2652